

Research paper

New insights into the evolutionary history of *Megacodon*: Evidence from a newly discovered speciesJun-Chu Peng^{a, b, c, 1}, Xiang-Guang Ma^{b, 1}, Yue-Hua Wang^a, Hang Sun^{b, *}^a School of Life Sciences, Yunnan University, Kunming 650091, China^b CAS Key Laboratory for Plant Diversity and Biogeography of East Asia, Kunming Institute of Botany, Chinese Academy of Sciences, Kunming 650201, China^c University of Chinese Academy of Sciences, Beijing 100049, China

ARTICLE INFO

Article history:

Received 6 April 2020

Received in revised form

28 May 2020

Accepted 28 May 2020

Available online 8 June 2020

Keywords:

Megacodon

Transcriptome

New species

Evolutionary pattern

Positive selection

ABSTRACT

Megacodon is an ideal genus to study speciation and ecological adaptation in the Sino-Himalayan region. The genus contains two species distributed at different elevations and in two separate areas. However, studies of this genus have long been impeded by a lack of fieldwork on one of its species, *Megacodon venosus*. In this study, we collected specimens of two *Megacodon* species and found an extraordinary new species of *Megacodon* in Lushui county of north-west Yunnan province, which we have since named *Megacodon lushuiensis*. We propose new species based on both morphological and molecular evidence. The finding of this new species emphasized the importance of ecological divergence in the divergence of *Megacodon stylophorus* and its parapatric low-elevation *Megacodon* species. To identify genetic determinants that underlie adaptations to different elevations, we characterized transcriptomes of the new species *M. lushuiensis*, which is distributed at low elevations, and *M. stylophorus*, which is distributed at high elevations. Comparative transcriptome analysis identified 8926 orthogroups containing single-copy genes, and 370 orthogroups containing significantly positively selected genes. The set of positively selected genes was enriched into 25 Gene Ontology terms, including “response to water deprivation”, “response to osmotic stress”, and “cellular response to external stimulus”. Our results provide new insights into how ecological adaptation and speciation occurred in *Megacodon* and highlight the role of heterogeneous habitats in the speciation of plants in the Sino-Himalayan region.

Copyright © 2020 Kunming Institute of Botany, Chinese Academy of Sciences. Publishing services by Elsevier B.V. on behalf of KeAi Communications Co., Ltd. This is an open access article under the CC BY-NC-ND license (<http://creativecommons.org/licenses/by-nc-nd/4.0/>).

1. Introduction

The Sino-Himalayan region is a temperate biodiversity hotspot with a high level of species endemism (Myers et al., 2000). Much of this diversity and endemism is attributed to the heterogeneous topography of the region and the diverse climates it supports (Shrestha et al., 2018). The formation of plant diversity in this region is synchronous with the uplift of the Qinghai-Tibet Plateau and has been intensified by climatic oscillations, especially the glacial–interglacial cycle during the Quaternary (Muellner-Riehl et al., 2019; Sun et al., 2017; Wen et al., 2014; Wu, 1988). The mechanisms of plant speciation and diversification in this region

are complicated and various (Muellner-Riehl et al., 2019; Wen et al., 2014). On the one hand, heterogeneous topography can create geographical barriers, which promote allopatric species divergence (e.g., Luo et al., 2017), and recent climatic oscillations can give rise to habitat fragmentation, which also interrupts the gene flow (e.g., Ma et al., 2017). On the other hand, divergent selection pressures across elevational gradients or heterogeneous habitats can also cause adaptive divergence in sympatry or parapatry (Funk et al., 2016), and even lead to adaptive radiation. This type of ecological divergence has been shown to be an essential speciation process for plants in the Sino-Himalayan region (e.g., Zhao et al., 2016).

Megacodon (Hemsl.) H. Smith is a small genus nested within a polytomy that contains *Swertia* L. and other genera in the Swertiinae (Chassot et al., 2001; Favre et al., 2016). However, *Megacodon* is morphologically distinct from other Swertiinae genera by having large campanulate flowers (Ho and Pringle, 1995). *Megacodon* contains two species: *Megacodon stylophorus* (C. B. Clark) H. Smith and *Megacodon venosus* (Hemsl.) H. Smith (Ho and Pringle, 1995).

* Corresponding author.

E-mail address: sunhang@mail.kib.ac.cn (H. Sun).

Peer review under responsibility of Editorial Office of Plant Diversity.

¹ These authors contributed equally to this work.

M. stylophorus is found at high elevations between 3000 and 4400 m a.s.l in western Sichuan, north-western Yunnan, southern Tibet of China, also in Bhutan, Nepal, and north-east India. *M. venosus* is endemic to China and is mainly found in Sichuan, western Hubei, and northern Chongqing at low to middle elevations between 600 and 2400 m a.s.l (Ho and Pringle, 1995). Previous studies of *Megacodon* have primarily focused on *M. stylophorus*, its phytochemistry (Liu et al., 2014), genetic diversity (Ge et al., 2005), embryology (Xue and Li, 2005), and breeding system (Meng et al., 2012). In contrast, *M. venosus* has been scarcely collected or reported. *M. venosus* was considered extinct until its rediscovery in 2007 by Prof. Zhen-Yu Li (Institute of Botany, the Chinese Academy of Sciences) in Northern Chongqing (Liu et al., 2014). Thus, it is vital to carry out investigations and conservation studies for this genus.

With rapid advances in next-generation sequencing (NGS), RNA-sequencing (RNA-seq) has become a more efficient approach for collecting gene sequences and studying ecological divergence in nonmodel organisms (Hudson, 2008; Strickler et al., 2012). For example, comparative transcriptome analysis can be used to identify candidate genes that underlie species diversification and adaptation, and then link these genes to specific biological processes (Voelckel et al., 2017). Previous studies have used genome- and transcriptome-based approaches to investigate adaptations to the high elevations of the Qinghai-Tibet Plateau region; however, few studies have examined these adaptations in plants, e.g., *Crucehimalaya himalaica* (Edgew.) Al-Shehbaz, O'Kane & R.A.Price (Qiao et al., 2016; Zhang et al., 2019), *Primula poissonii* Franchet and *Primula wilsonii* Dunn (Zhang et al., 2013), *Cupressus gigantea* W. C. Cheng & L. K. Fu and *C. duclouxiana* Silba (Ma et al., 2019), *Salix brachista* C. K. Schneider (Chen et al., 2019), *Eutrema heterophyllum* (W. W. Smith) H. Hara and *E. yunnanense* Franchet (Guo et al., 2018), *Notopterygium incisum* C. C. Ting ex H. T. Chang (Jia et al., 2019). For these studies, Gene Ontologies (GOs) of biotic and abiotic stress often provide novel insights into the local adaptation and species divergence in the extreme environments of the Qinghai-Tibet Plateau region.

During field investigation in 2017, we found a putative new species of *Megacodon* in Lushui county of north-west Yunnan at 1700 m a.s.l. This Lushui *Megacodon* has similar morphology and habitat as that of *M. venosus*; however, the Lushui *Megacodon* and *M. venosus* have extraordinarily disjunctive distributions. The new record of *Megacodon* from Lushui implies that the evolutionary history of this genus may be more complicated than previously thought. Two species co-occur in the Nushan Mountains, yet at different elevations. Furthermore, these observations suggest that the divergence of these *Megacodon* species may have been the result of both ecological divergence and allopatric speciation.

In this study, we described a new species of *Megacodon* from Lushui (Fig. 1) and determined its phylogenetic relationships within *Megacodon*. To identify genetic signatures of adaptive evolution to different elevations, we compared the transcriptome of *M. stylophorus*, which is distributed at high elevations, with that of the new species *Megacodon lushuiensis*, which is distributed at low elevations.

2. Materials and methods

2.1. Material collection

We sampled a total of 12 samples of *M. stylophorus* from different sites in Tibet and Yunnan, two samples of *M. venosus* from Chongqing, and two samples of the putative new species from Lushui, Yunnan (Fig. 1 and Table S1). Leaves were collected and dried in silica gel for DNA extraction. Specimens were deposited at the herbarium of Kunming Institute of Botany, Chinese Academy of

Sciences (KUN). Flower organs of the *Megacodon* species from Lushui and *M. stylophorus* from Daxueshan Mountain were sampled by liquid nitrogen and stored at -80°C for RNA-seq. Each sample was obtained from one individual.

2.2. DNA extraction, PCR amplification, and sequencing

The Plant Genomic DNA Kit (Tiangen Biotech, Beijing, China) was used to extract total genomic DNA following the manufacturer's protocol. The nuclear ribosomal internal transcribed spacer (nrITS) and two chloroplast markers, *atpB-rbcL*, and *trnL-trnF*, were amplified and sequenced following the protocols of previous studies (Favre et al., 2016; Matuszak et al., 2016). Primers used in this study for *atpB-rbcL*, *trnL-trnF*, and the nrITS region were the same as those used in previous studies (see Hoot et al., 1995; Taberlet et al., 1991; Grudinski et al., 2014 for the nrITS region). The 25 μL volume polymerase chain reactions (PCRs) contained 1.0 μL of genomic DNA (20 ng/ μL), 0.3 μL of each primer (10 μM), 12.5 μL *Ex Taq* Version 2.0 (Takara, Dalian, China), and 10.9 μL of double-distilled H_2O . PCRs were performed in a C1000 Touch™ Thermal Cycler (Bio-Rad, Hercules, CA, USA), with initiation at 95°C for 2 min followed by 35 cycles of denaturation at 95°C for 1 min, primer annealing at $53\text{--}56^{\circ}\text{C}$ for 1 min, primer extension at 72°C for 1 min and a final extension step at 72°C for 10 min. Alignments and subsequent manual adjustment were performed in BioEdit 7.2.5 (Hall, 1999) by using the multiple alignment software ClustalW (Thompson et al., 1994).

2.3. Phylogenetic analyses

Maximum likelihood (ML) and Bayesian inference (BI) approaches were used for phylogenetic tree reconstruction with combined sequences from nrITS, *atpB-rbcL*, and *trnL-trnF*. Three *Potalia* Aubl. and three *Lisianthus* P. Browne species were set as outgroups (Table S2). In addition, 11 *Gentiana* L. species and 29 *Swertia* species were included as closely related genera (Table S2). ML analyses were performed on the CIPRES Science Gateway (www.phylo.org; Miller et al., 2010) through RAXML-HPC2 v.8.2.8 (Stamatakis, 2014) with 1000 bootstrap replicates. The best-fitting nucleotide substitution model for BI analyses was GTR + G, selected using the Akaike information criterion (AIC) in jModeltest 2.1.7 (Darriba et al., 2012). BI analyses were also performed on CIPRES using MrBayes v.3.2.6 (Ronquist et al., 2012) on XSEDE with the following settings: ngen = 10,000,000, samplefreq = 1000, printfreq = 1000 and sumt burnin = 2500.

2.4. Climatic data analysis

Our fieldwork identified 15 precise locations where *Megacodon* is distributed. We used the 'raster' package to extract 19 bioclimatic variables for these sites from WorldClim (<http://www.worldclim.org>; Hijmans et al., 2005). Principal component analysis (PCA) of these environmental factors was performed by the *dudi.pca* function of the package 'ade4' in R 3.5.1 (R Core Team, 2018). We conducted paired two-tailed t-tests in Microsoft® Excel® 2016 (Microsoft Company, USA) to characterize factors that diverged between *M. stylophorus* and the other two *Megacodon* species (including the suspected new species from Lushui).

2.5. Transcriptome sequencing and functional annotation

TRIzol reagent (Sigma–Aldrich) was used to extract total RNA of samples following the manufacturer's instructions. A total amount of 3 μg of RNA per sample was used to construct a cDNA library with a fragment length range of 250–300 bp. The cDNA libraries were

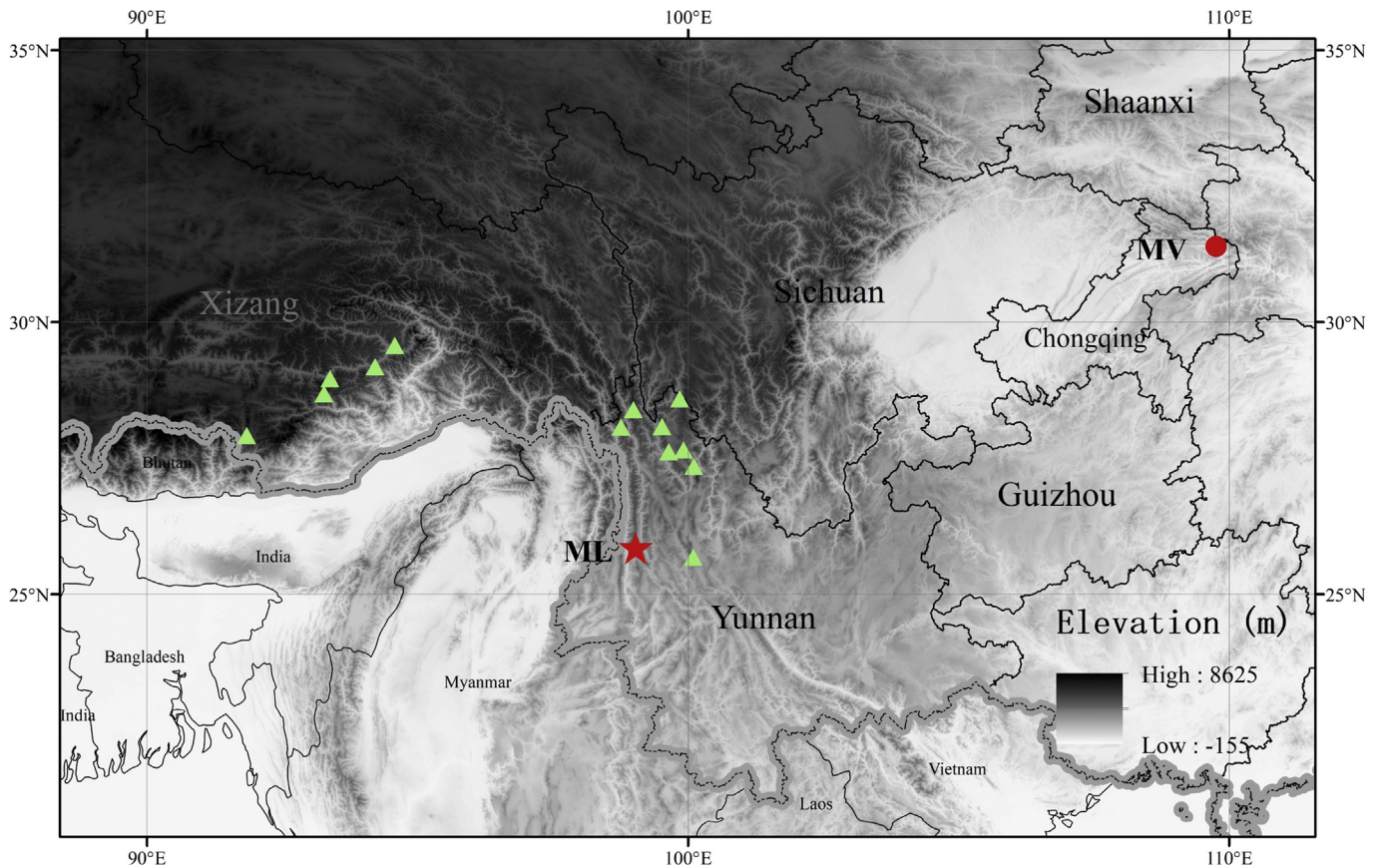


Fig. 1. Geographic distributions of *Megacodon* samples. The red pentagram represents the putative new species (ML) in Lushui county, north-west Yunnan. The green triangles show the sampled natural populations of *M. stylophorus*. The red dot represents the *M. venosus* (MV) population from northern Chongqing.

created with NEBNext® Ultra™ RNA Library Prep Kit for Illumina® (NEB, USA), following the manufacturer's recommendations. Illumina HiSeq 2500 was used for sequencing the library preparations, and paired-end reads were generated. Library preparation and Illumina sequencing were performed at Novogene Bioinformatics Technology Co., Ltd., Beijing, China (www.novogene.cn). Clean data was obtained by trimming read adapter sequences, and filtering low-quality reads from raw data. De novo assembly of each individual was accomplished using the Trinity program (Raychowdhury et al., 2011) with `min_kmer_cov` set to 2, and all other parameters set to default.

Functions of all assembled unigenes were annotated based on the following databases: Nr (NCBI non-redundant protein sequences); Nt (NCBI non-redundant nucleotide sequences); Pfam (Protein family); KOG/COG (Clusters of Orthologous Groups of proteins); Swiss-Prot (A manually annotated and reviewed protein sequence database); KO (KEGG Ortholog database); and GO (Gene Ontology).

2.6. Homologous gene identified and positive selection analysis

We used OrthoFinder software v. 2.2.7 (Emms and Kelly, 2018, 2015) to identify homologous gene clusters (orthogroups). OrthoFinder was run with multiple sequences alignment (MSA) for gene tree inference and RAxML for tree inference method (-T ramx1 -M msa). Orthogroups of single-copy genes (1:1 orthologs) were obtained for substitution rates estimation. Each orthogroup was aligned by Prank (Löytynoja and Goldman, 2005) at the codon level (with options "-F -codon"). To estimate a general evolutionary

pattern of selective pressure for the two species, codeml program from PAML 4.9 (Yang, 2007) was used to calculate the d_N , d_S and d_N/d_S with the free ratio model (model = 2, NSsites = 0) and ML pairwise alignment (runmode = -2). To reduce false-positive findings in subsequent evolutionary analyses, genes with length less than 150 bp, $d_S < 0.001$ (to avoid a very large d_N/d_S ratio) and $d_S > 0.1$ (to avoid suspicious paralogs) were discarded (Bustamante et al., 2005; Sun et al., 2018; Zhang et al., 2013).

Positive selection genes ($d_N/d_S > 1$) were used as the test set for the GO enrichment analysis, which was performed on web-based KOBAS software (Xie et al., 2011) by Fisher's exact test, while whole single-copy genes were selected as the background set. Significant enriched GO terms ($P < 0.05$) were selected and further analyzed using REVIGO (<http://revigo.irb.hr/>; Supek et al., 2011) to investigate in-depth GO similarities.

3. Results

3.1. Morphological comparisons and molecular variation

Comparative analysis of morphological traits indicates that the *Megacodon* species from Lushui is closely related to *M. venosus* (Fig. 2 and Table 1). The *Megacodon* species from Lushui is similar to *M. venosus* by its narrow leaf blades shape, calyx shape and the existence of glands at the base of calyx, but differs from *M. venosus* by its taller and thinner plant, lower stem leaf blades elliptic-spathulate to elliptic-obovate (vs. elliptic-lanceolate), middle to upper stem leaf blades veins 3–5 (vs. 5–7), 11–15-flowered thyrses (vs. 7–11 flowered), and dense glands at the 1/3 base of the calyx

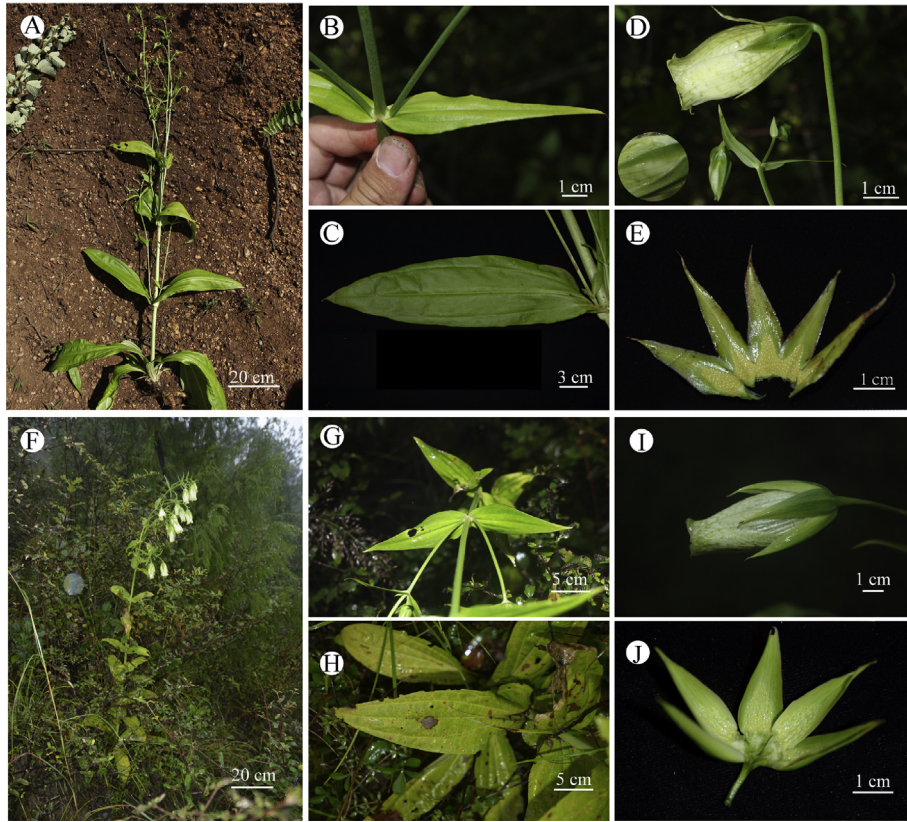


Fig. 2. Photographs of the putative new species *Megacodon lushuiensis* (A–E) and *Megacodon venosus* (F–J). A and F. Habitat and habit. B and G. Upper stem leaf blades. C and H. Middle stem leaves. D and I. Flower. E and J. Calyx. (A–D photographed by Jun-chu Peng; E–J photographed by Yi Yang).

(vs. sparse glands at the 1/2 base of the calyx). Two individuals from Lushui and two individuals from *M. venosus* differed by a total of eleven nucleotide substitutions and six insertions/deletions in the alignment dataset (including ITS, *atpB-rbcL*, *trnL-trnF*, Table S3).

3.2. Phylogenetic relationships of *Megacodon*

The data set of phylogenetic analyses comprised 62 accessions with 2383 characters. Because the topologies of phylogenetic trees

Table 1

Comparison of distribution and morphological characters of *Megacodon lushuiensis*, *M. venosus*, and *M. stylophorus* based on field observation and description from *Flora of China* (Ho and Pringle, 1995).

		<i>M. lushuiensis</i>	<i>M. venosus</i>	<i>M. stylophorus</i>
Habit		Plants 130–240 cm tall	Plants 45–85 (–180) cm tall	Plants 30–60 (–100) cm tall
Stems		Basal to middle stems erect, terete, 1.1–1.8 cm in diam at base; upper stems slim 3–9 mm in diam	Stems erect, terete, stout, 1–1.5 cm in diam	Stems erect, terete, stout, 1–1.5 cm in diam
Lower stem leaf blades	shape	elliptic-spathulate to elliptic-obovate	elliptic-lanceolate	elliptic to ovate-elliptic
	veins	5–7	5–7	7–9
Middle stem leaf blades	shape	elliptic-lanceolate to lanceolate	elliptic-lanceolate	elliptic to ovate-elliptic
	size	15–45 × 5–14 cm	10–30 × 3–6 cm	7–22 × 3–9 (–14) cm
	veins	3–5	5–7	7–9
Upper stem leaf blades	shape	linear-lanceolate to linear	linear-lanceolate	ovate-lanceolate
	size	5–10 × 1.1–1.5 cm	5–7 × 0.7–1.2 cm	5–10 × 1.2–3
	veins	3–5	5–7	7–9
Thyrses		11–15-flowered	7–11-flowered	2–8-flowered
Pedicel		3–9 cm	2.5–6 cm	3–6 (–16) cm
Calyx	lobes shape	elliptic-lanceolate, apex acuminate	elliptic-lanceolate, apex acuminate	oblong-spatulate, apex obtuse.
	lobes length	1.7–3.6 cm	2.5–3 cm	2–2.6 cm
	tube length	4–6 mm	2–3 mm	6–8 mm
	Nectary	dense pustulose glands at the base ca. 1/3	Sparse pustulose glands at the base ca. 1/2	No glands
Corolla	size	ca. 5–7 × 4–5 cm	5–6 × 6–7.5 cm	5–7 × 4–5 cm,
	lobes shape	oblong-spatulate	oblong-spatulate	oblong-spatulate
	lobes length	4–5.8 cm	4–5 cm	4–6 cm
Anthers		8–11 mm	7–10 mm	1–1.2 cm
Style		ca. 1.7–2.0 cm	1.5–1.8 cm	1.5–1.8 cm
Phenology	Fl. and fr.	Sep. to Nov.	Sep. to Nov.	Jun. to Sep.
Distribution		1700 m, NW Yunnan	600–2400 m. W Hubei, Sichuan, N Chongqing	3000–4400 m. S Sichuan, SE Tibet, NW Yunnan [Bhutan, NE India, Nepal]

from ML and BI analyses were mostly identical, only the ML tree is shown with the posterior probabilities (PP) from BI analysis (Fig. 3). Phylogenetic inference showed that *Megacodon* is most likely a monophyletic group (ML-BS = 100/BI-PP = 1.00 in Fig. 3). Twelve accessions of *M. stylophorus* from Tibet and Yunnan formed a well-supported clade (96/1.00). In comparison, two accessions of *M. venosus* from Chongqing and two accessions from Lushui formed the other clade of *Megacodon*. The population of *M. venosus* and the species from Lushui each formed a monophyletic clade in this branch.

3.3. Taxonomic treatment

According to both morphological and molecular evidence, as well as the extraordinary disjunctive distribution with *M. venosus*, we propose the *Megacodon* plants from Lushui as a new species here.

***M. lushuiensis* J. C. Peng & H. Sun sp. nov.** (Fig. 2A–E, and Fig. 4).

Holotype. China, Yunnan Province: Laowo Xiang, Lushui County, on the hillside, 1700 m a.s.l, 25.85°N, 99.03°E, flowering, 21 September 2017, J. C. Peng & L. Sun PM001 (KUN).

Paratype. The same locality, flowering and fruiting, 7 November 2017, J. C. Peng, L. Sun & Z. Chen PM002 (KUN).

Description. Plant perennial, herbaceous ca. 130–240 cm tall. Basal to middle stems erect, terete, 1.1–1.8 cm in diam at base; upper stems slim, 3–9 mm in diam. Lower stem leaves elliptic-spathulate to elliptic-obovate, base cuneate and decurrent, veins 5–7 and arcuate; middle stem leaves elliptic-lanceolate to lanceolate, apex acuminate, 15–45 × 5–14 cm, veins 3–5 and arcuate; upper stem leaves linear-lanceolate to linear, 5–10 × 1.1–1.5 cm, veins 3–5 and arcuate. Thyrses 11–15-flowered. Pedicel 3–9 cm. Calyx campanulate, 1.7–3.6 cm, tube 4–6 mm; lobes elliptic-lanceolate, apex acuminate, dense pustulous glands at the base

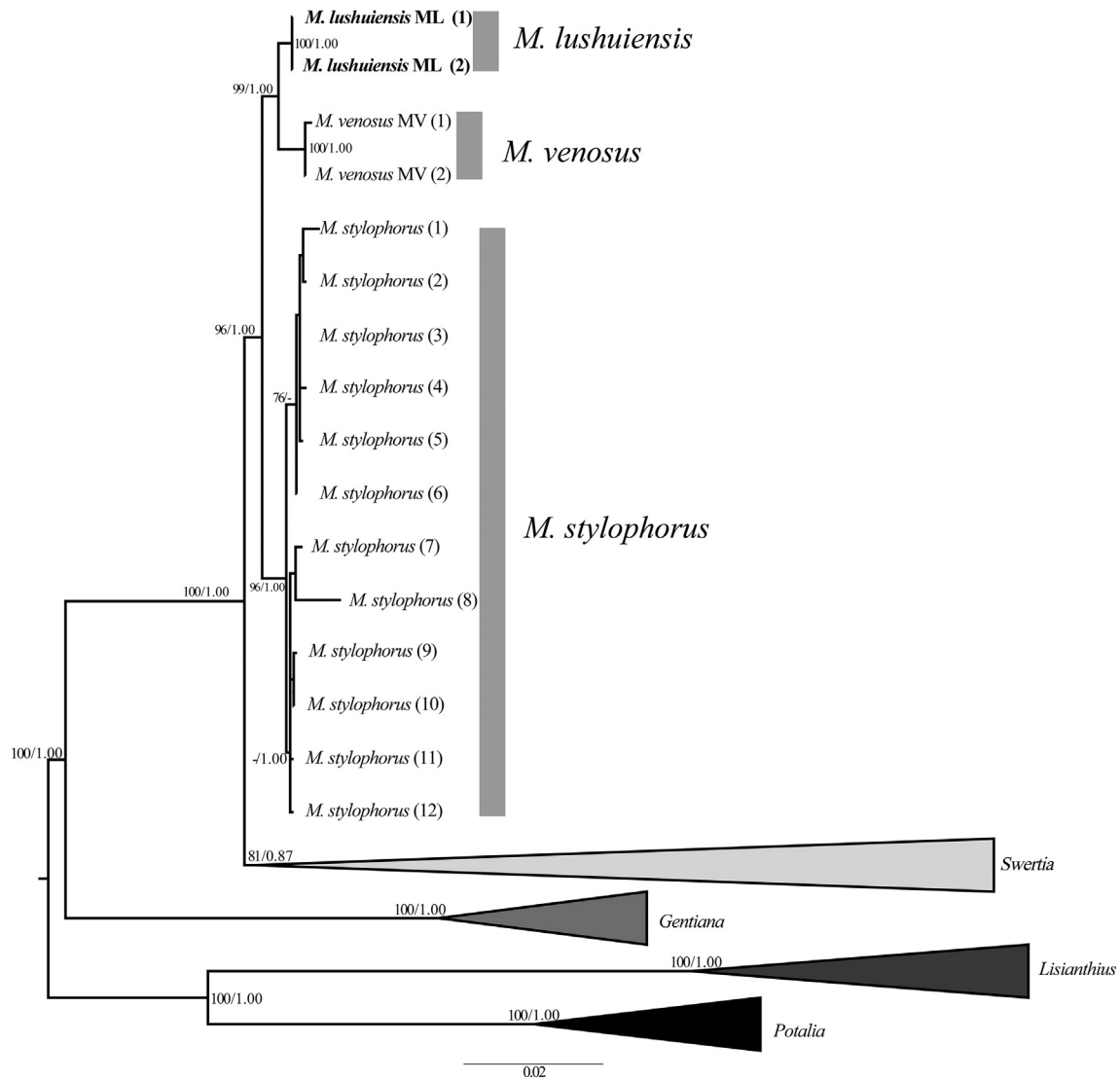


Fig. 3. Molecular phylogeny of *Megacodon* and four other genera (*Swertia*, *Gentiana*, *Lisianthus*, and *Potalia*) based on nrITS, *atpB-rbcL*, and *trnL-trnF* sequences. ML bootstrap support values (BS) and Bayesian posterior probabilities (PP) are indicated on nodes and separated by a slash. Values for nodes with less than 75 (BS) or 0.85 (PP) are not shown. *M. lushuiensis* are shown bold.

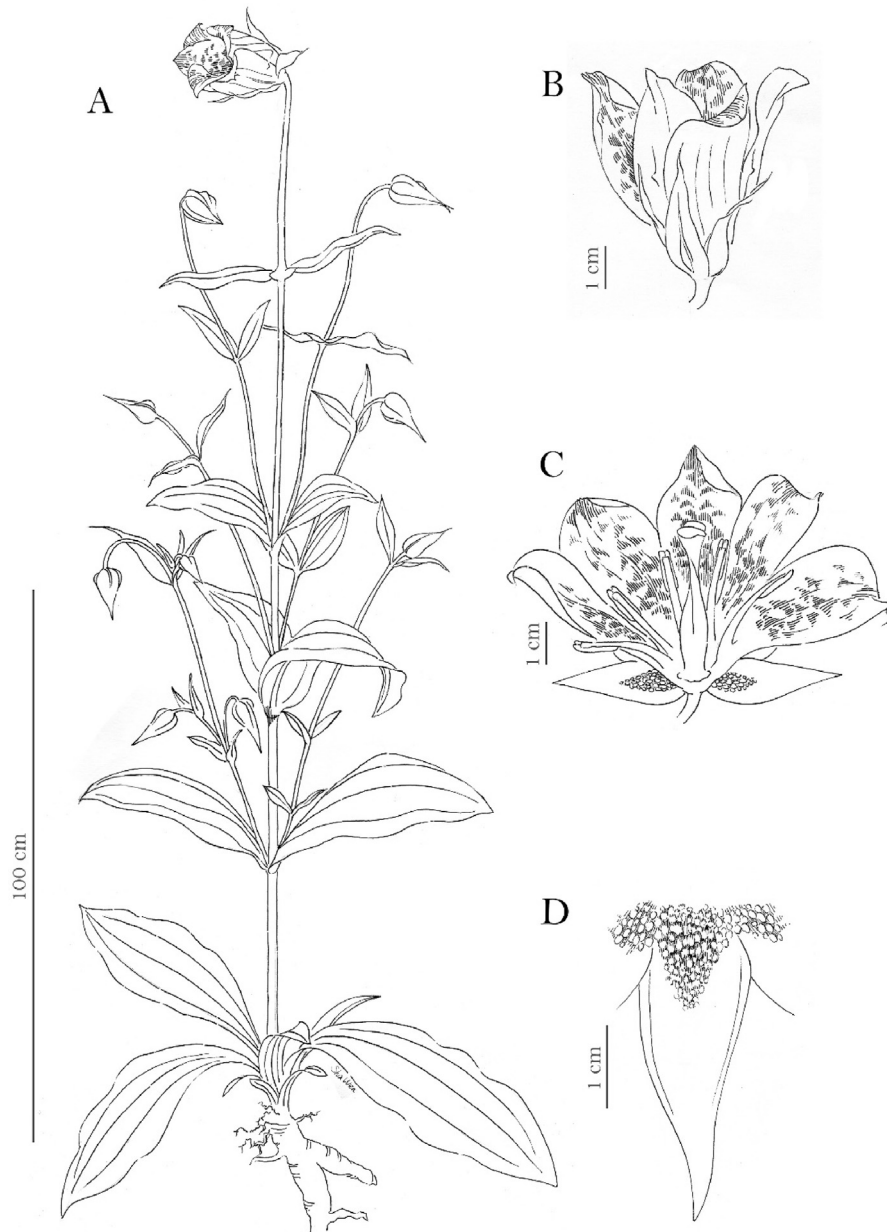


Fig. 4. *Megacodon lushuiensis* J. C. Peng & H. Sun *sp.nov.* (drawn by Wen Sha). A. Habit B. Flower C. Opened corolla lobes D. Partial calyx.

ca. 1/3. Corolla white to pale yellow, with green veins, ca. 5–7 × 4–5 cm, tube 8–10 mm; lobes oblong-spatulate, 4–5.8 cm, apex rounded. Filaments flat and linear, 2.2–2.8 cm, alternate with lobes; anthers oblong-quadrate, 8–11 mm; Capsule ovoid-ellipsoid, 1.7–2.0 cm.

Phenology. Flowering and fruiting from Sep. to Nov.

Distribution and habitat. *M. lushuiensis* was found in Laowo Xiang of Lushui County, north-west Yunnan, south-west China (Fig. 1), growing on hillsides (north-west slope) and under shrub at ca. 1700 m a.s.l.

Conservation status. *M. lushuiensis* is only known from one population in Lushui county (criterion B2a), with an area of occupancy estimated to be less than 500 km² (criterion B2b (i, ii)). The habitat of this population is near to cultivated field (less than 2 km) and suffering from invasive plants such as *Ageratina adenophora*

(criterion B2b (iii)). The new species should be regarded as “Endangered” based on the IUCN (2012) criteria.

Etymology. The specific epithet refers to the type locality, Lushui County of Yunnan Province, in China.

3.4. Climatic niche

PCA of 19 bioclimatic variables indicated clear climate niche differentiation between 13 *M. stylophorus* sites, one *M. venosus* site, and one *M. lushuiensis* site (Fig. 5). The first two PCs identified two climatic groups and explained 59% and 26.2% of the total variation, respectively (Fig. 5). The climatic niche of *M. lushuiensis* is closer to the population of *M. venosus* from Chongqing, whereas 13 sites of *M. stylophorus* formed another group. Among these 19 bioclimatic variables, 12 bioclimatic variables (BIO1, BIO5, BIO6, BIO8–BIO12, BIO14, BIO15, BIO17, and BIO19) showed significant differences

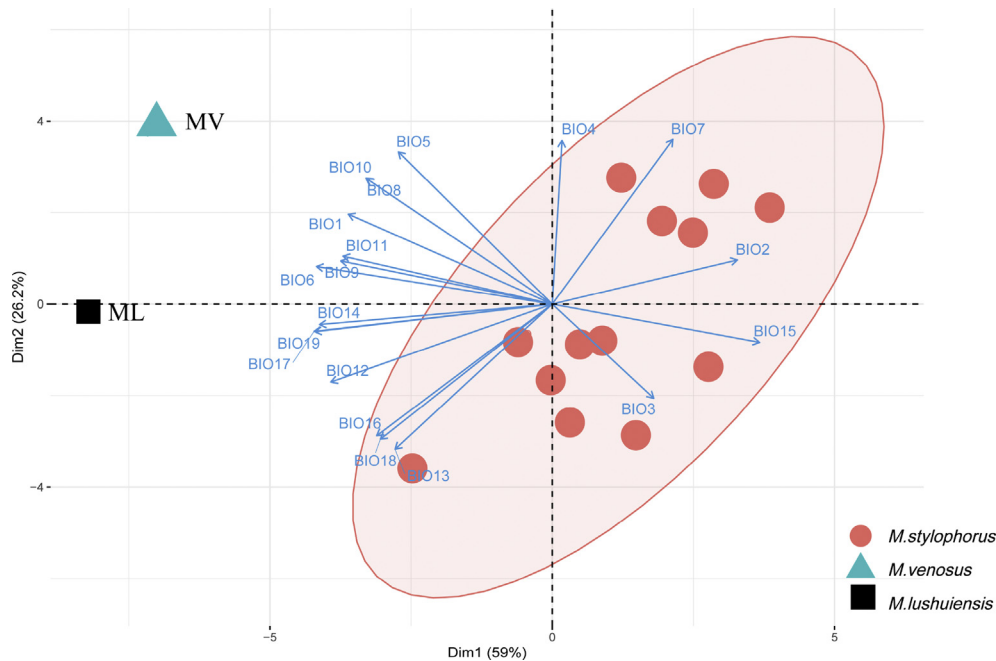


Fig. 5. PCA analysis of bioclimatic factors of the putative new species (*M. lushuiensis* black square), *M. stylophorus* (red dots), and *M. venosus* (blue triangle). Each arrow represents a projection of a bioclimatic variable.

between *M. stylophorus* and the other two species ($P < 0.01$; Table S4).

3.5. Overview of RNA-seq analysis

We generated 55.2 and 55.3 million clean reads of RNA-seq data for *M. lushuiensis* and *M. stylophorus*, with a total size of 8.28 and 8.30 Gb, respectively (NCBI GenBank accession number: SRR11743766, SRR11743765 and Table 2). The median unigene length for *M. lushuiensis* after de novo assembly was 981 bp, with an N50 length of 2043 bp. The median unigene length for *M. stylophorus* was 1018 bp, with an N50 length of 2058 bp. A total of 24,086 unigenes from *M. lushuiensis* and 23,262 unigenes from *M. stylophorus* were annotated in at least one database with a significant match ($e\text{-value} < 10^{-5}$).

3.6. Orthogroups identified and positive selection analysis

In this study, a total of 20,679 and 20,471 unigenes were detected in *M. lushuiensis* and *M. stylophorus*, respectively, and 23,611 orthogroups were identified. Among these, 8926 orthogroups contained putative one-to-one single-copy genes between two species. To detect genes that are involved in ecological adaptation to high elevations, d_N , d_S , and d_N/d_S ratio of single-copy genes were calculated by PAML. A peak of d_S distribution between *M. stylophorus* and *M. lushuiensis* was observed at 0.0411 ± 0.0210 (Fig. 6A). The d_N/d_S of most genes was less than one (Fig. 6B), which

indicates purifying selection. Only 370 single-copy genes were identified as positively selected genes (PSGs, $\omega > 1$) between two species.

In enrichment analyses, the 370 positively selected genes were designated as the test sets, and 7749 single-copy genes ($0.001 < d_S < 0.1$) were designated as the background set. Twenty-five GO categories were annotated to 49 pairs of positively selected genes, which were overrepresented (Fisher's exact test, $p < 0.05$) in the test sets (Table 3) by GO enrichment analysis in the KOBAS website. Then based on GO similarities, five clusters of biological processes were shown in the REVIGO treemap (Fig. 6C). A majority of biological processes in treemap were found to be related to specific adaptation traits, such as response to water (11 PSGs), regulation of response to osmotic (3 PSGs), cellular response to nutrient levels (7 PSGs), and cellular response to external stimulus (7 PSGs) (Fig. 6C, Table 3 and Table S5).

4. Discussion

4.1. New insights into the evolutionary history of *Megacodon*

In this study, we described a new species of *Megacodon*, *M. lushuiensis*, and determined the phylogenetic relationships among *Megacodon* species. The three existing *Megacodon* species formed a well-supported monophyletic clade (Fig. 3). All samples of *M. stylophorus* formed a monophyletic clade. Furthermore, in our phylogenetic tree, *M. lushuiensis* is closely related to *M. venosus*,

Table 2
Statistics of clean data and unigenes of RNA-seq.

Species	Statistics of clean data						Frequency distribution of unigene lengths						
	Clean Reads	Clean Bases (G)	Error (%)	Q20 (%)	Q30 (%)	GC Content (%)	Total number	min length (bp)	mean length (bp)	median length (bp)	max length (bp)	N50 (bp)	total nucleotides (bp)
<i>M. lushuiensis</i>	55,224,736	8.28	0.03	96.3	90.2	43.2	35,573	301	1400	981	16,580	2043	49,784,866
<i>M. stylophorus</i>	55,301,198	8.30	0.03	96.7	91.0	43.5	33,202	301	1420	1018	15,568	2058	47,132,153

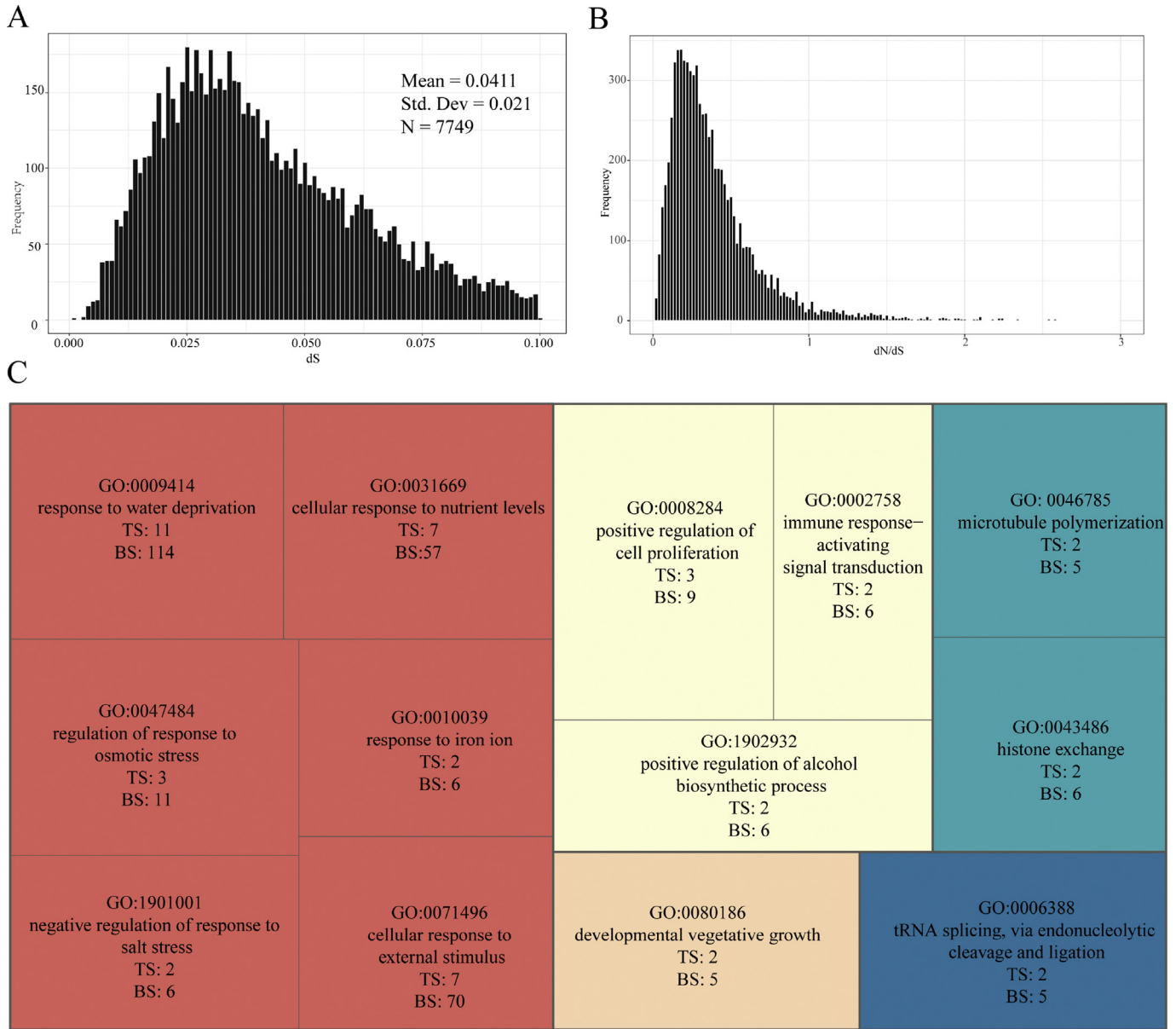


Fig. 6. The d_S (A) and d_N/d_S ratio (B) distribution of orthologs between *M. stylophorus* and *M. lushuiensis*. REVIGO treemap summarizing GO biological process categories over-represented regarding ecological divergence of *M. lushuiensis* and *M. stylophorus* (C). KOBAS was used to identify GO biological processes that were overrepresented at p-values (Fisher's exact test) ≤ 0.05 . Similar colors indicate semantic similarity related to a similar functional category. The size of each rectangle is proportional to the p-value (Fisher's exact test) for that category. TS: frequency in the test set; BS: frequency in the background set.

Table 3
Partial list of positively selected genes related to ecological adaptation.

Orthologs	<i>Arabidopsis thaliana</i> gene accession	Description	d_N/d_S
OG0007681	AT1G32230	RCD1, WWE protein–protein interaction domain protein family	1.99
OG0010334	AT3G17810	PYD1, pyrimidine 1	1.31
OG0002624	AT2G39550	PGGT-1, Prenyltransferase family protein	1.05
OG0009542	AT1G11755	LEW1, Undecaprenyl pyrophosphate synthetase family protein	1.10
OG0009326	AT3G08040	FRD3, MATE efflux family protein	1.12
OG0008777	AT4G33630	EX1, UvrB/UvrC domain protein	1.15
OG0009854	AT3G63060	EDL3, EID1-like 3	1.15
OG0003758	AT1G06770	DRIP1, DREB2A-interacting protein 1	1.16
OG0008137	AT4G36020	CSDP1, cold shock domain protein 1	1.15
OG0009134	AT5G28770	BZO2H3, bZIP transcription factor family protein	1.75
OG0004371	AT3G62420	BZIP53, basic region/leucine zipper motif 53	1.42
OG0006371	AT3G48170	ALDH10A9, aldehyde dehydrogenase 10A9	1.51

which is consistent with the morphological similarity between these two species. The phylogenetic relationship between *Megacodon* and four other lineages (*Potalia*, *Lisianthus*, *Gentiana*, and *Swertia*) is congruent with previous studies (Favre et al., 2016). Although sharing many morphological similarities, *M. lushuiensis* can be easily distinguished from *M. venosus* by its leaf blade, inflorescence, extrafloral nectaries, and more. Importantly, the extrafloral nectaries in the basal portion of the calyx were neglected in previous morphological descriptions of *M. venosus*. The extrafloral nectaries of *M. venosus* and *M. lushuiensis* not only secrete nectar but also cover the petal and make it sticky (Fig. 2D, E, I, and J). We speculate that in addition to attracting ants to participate in ant-plant mutualisms, the secretions from *M. venosus* and *M. lushuiensis* extrafloral nectaries may directly participate in the protection of the flowers (Marazzi et al., 2013).

The exact distribution of *M. lushuiensis* in north-west Yunnan indicates that the most recent common ancestor of *M. lushuiensis* and *M. venosus* may occupy a more extensive area, from west Yunnan to central China. In the past, *Megacodon* populations from the Nujiang River valley may have been connected to *M. venosus* populations from central China through the eastern edge of the Qinghai-Tibet Plateau region or the Yunnan-Guizhou Plateau. The current fragmented distribution of this species pair may be the result of a vicariance event closely related to the climatic changes of the Sino-Himalayan region and its low reproductive capacity. Because of its humid climate and large elevational gradient, the Nujiang River valley harbors many distinct species that are identical to or sister to species in central or south China, such as *Ichtyoselmis macrantha* (Oliver) Lidén, *Ypsilandra* Franch., *Asteropyrum peltatum* (Franch.) Drumm. ex Hutch. The large elevational gradient and complex climate conditions in Nushan Mountain should provide more ecological opportunities for the maintenance of relict populations or species. Despite this, the fragmented distribution pattern of *M. venosus* and *M. lushuiensis* is still rare and may have important significance in biogeographical studies.

The occurrence of *M. lushuiensis* in north-west Yunnan also alters our understanding of the divergence of *M. stylophorus* and related species. Speciation of *M. venosus* and *M. stylophorus* was previously thought to have occurred through allopatric speciation, similar to that of *Pleurospermum hookeri* C. B. Clarke and *P. giraldii* Diels, which have a fragmented distribution between central China and the Qinghai-Tibet Plateau region (Bai et al., 2015). However, the fragmented distribution of *M. lushuiensis* and *M. stylophorus* occur at different elevations along the Nushan Mountain, suggesting that ecological differentiation may have played an important role in their divergence.

4.2. Functions under positive selection between *M. lushuiensis* and *M. stylophorus*

To further investigate why *M. lushuiensis* and *M. stylophorus* occupy distinct ecological niches along an elevational gradient, we used comparative transcriptome analysis. The majority of genes identified by GO enrichment of *M. lushuiensis* and *M. stylophorus* function in response to water deprivation (GO:0009414) and other external stimuli (e.g., GO:0047484 and GO:0071496) (Fig. 6C). These findings suggest that genes that respond to the environment may have been triggered by natural selection during ecological adaptation (Table 3). However, unlike many other alpine plants, especially alpine scree plants (Chen et al., 2019; Guo et al., 2018; Jia et al., 2019; Zhang et al., 2019), *M. stylophorus* does not appear to have adapted to high radiation. This may be because *M. stylophorus* grows in the forest or scrub habitat. Analysis of climatic variables

revealed that *M. stylophorus* favors the colder and higher climatic drought conditions of high elevations (Fig. 5 and Table S1). In contrast, field observations indicate that *M. lushuiensis* prefers to grow in drier soil conditions such as semi-humid hillsides at low elevations (Fig. 2A). Habitat differentiation between these two species may have led some populations to experience water deficiency at different periods, which can influence plant growth and development. Our transcriptome analysis identified several genes (e.g., *PGGT-1*, *ALDH10A9*, and *EDL3*) under positive selection that is directly involved in water deprivation and hormone signaling pathways (Johnson et al., 2005; Koops et al., 2011; Missihoun et al., 2014). *DRIP1* is a negative regulator in drought tolerance-responsive gene expression that was also found to be under positive selection (Qin et al., 2008). Our study also found that the following genes were under positive selection: *LEW1*, which response to endoplasmic reticulum stress, drought, and dark-induced senescence by catalyzing dolichol biosynthesis (Zhang et al., 2008); *RCD1*, which is involved in the regulation of stomatal conductance and the flavonoid accumulation pathway (Ahlfors et al., 2004; Suvorov et al., 2017); and *CSDP1*, which contains a cold shock domain and is involved in cold and salt stress responses (Yang and Karlson, 2013). The functions of these homologous genes emphasize that the genetic pathways that regulate efficient water use may have been important drivers of the divergence of *M. lushuiensis* and *M. stylophorus*.

Under a short growing season in the alpine region, *M. stylophorus* also require proper phenological responses. Our transcriptome analysis identified several genes that may play roles in these phenological responses. For example, in addition to its response to water deprivation, *CSDP1* can also regulate seed germination (Yang and Karlson, 2013). Furthermore, *bZIP53* is an enhancer for seed maturation gene transcription (Alonso et al., 2009), while *BZOZH3* (also known as *bZIP63*) is involved in the regulation of a circadian oscillator gene *PRR7* (Frank et al., 2018). The correct circadian clock guarantees that plants have photosynthetic advantages and can accurately anticipate environmental changes (Dodd et al., 2014, 2005). These homologous genes may strengthen the ability of *M. stylophorus* to respond to habitat-specific variability. Similarly, *EX1* and *FRD3*, which were identified in our analysis, may help *M. stylophorus* tolerate higher oxidative stress and iron deficiency that result from radical-initiating factors at high elevations (Dogra et al., 2019; Lei et al., 2014), especially at the end of the growing period (Sakata et al., 2006). Overall, adapting to extreme environments (such as climatic drought, oxidative stress, and low temperature) in Sino-Himalayan regions may play an important role in the speciation of *Megacodon*.

5. Conclusion

In this study, we used field observations in conjunction with morphological and molecular data to propose a new *Megacodon* species from the Nujiang River valley, *M. lushuiensis*. The discovery of this species calls attention to the importance of ecological divergence between *M. stylophorus* and low-elevation *Megacodon* species. We also presented the phylogenetic position *M. venosus* for the first time and described a neglected trait in this species (sparse glands at 1/2 base of the calyx). Although population genetic and genomic studies are essential to understanding the demographic and divergence history of *Megacodon*, our analysis of the transcriptomes of *M. stylophorus* and *M. lushuiensis* provide valuable resources for the future genomic research and general insight into how ecological divergence occurred between these two *Megacodon* species. *M. venosus* and *M. lushuiensis* are both extremely rare in the

field; we, therefore, recommend that conservation efforts be carried out timely and properly for these two species.

Author contributions

HS, XGM and YHW conceived and designed experiments. JCP performed field investigations, analyzed the data, and wrote the manuscript. XGM and HS revised the manuscript.

Declaration of Competing Interest

We declare that we do not have any commercial or associative interest that represents a conflict of interest in connection with the work submitted.

Acknowledgments

This study was supported by the Key Projects of the Joint Fund of the National Natural Science Foundation of China (U1802232), the Second Tibetan Plateau Scientific Expedition and Research (STEP) program (2019QZKK0502). Thanks to Si-Rong Yi (Chongqing Three Gorges Medical College) and Wei Zhang for providing valuable distribution information, Sha Wen for her line drawing of the new species, Ti-Cao Zhang (Yunnan University of Chinese Medicine) and Yan-Ting Hu for useful advice on RNA-seq analysis. We also appreciate the help of Jian Wen Zhang, Zhuo Zhou, Yang Niu, Yi Yang, Lu Sun, Zhe Chen, Bo Xu (Southwest Forestry University), Hong-Liang Chen, Li-Shen Qian, and Yong-Zeng Zhang during fieldwork.

Appendix A. Supplementary data

Supplementary data to this article can be found online at <https://doi.org/10.1016/j.pld.2020.05.003>.

References

- Ahlfors, R., Lång, S., Overmyer, K., et al., 2004. *Arabidopsis* RADICAL-INDUCED CELL DEATH1 belongs to the WWE protein–protein interaction domain protein family and modulates abscisic acid, ethylene, and methyl jasmonate responses. *Plant Cell* 16, 1925–1937.
- Alonso, R., Oñate-Sánchez, L., Weltmeier, F., et al., 2009. A pivotal role of the basic leucine zipper transcription factor bZIP53 in the regulation of *Arabidopsis* seed maturation gene expression based on heterodimerization and protein complex formation. *Plant Cell* 21, 1747–1761.
- Bai, X., Ma, X.G., Gao, Y.D., et al., 2015. Intraspecific differentiation of *Pleurospermum hookeri* (Apiaceae), and its interspecific relationships with two close relatives in the genus *Pleurospermum*. *J. Systemat. Evol.* 53, 308–320.
- Bustamante, C.D., Fedel-Alon, A., Williamson, S., et al., 2005. Natural selection on protein-coding genes in the human genome. *Nature* 437, 1153–1157.
- Chassot, P., Nemomissa, S., Yuan, Y.M., et al., 2001. High paralogy of *Swertia* L. (Gentianaceae) in the Gentianella-lineage as revealed by nuclear and chloroplast DNA sequence variation. *Plant Systemat. Evol.* 229, 1–21.
- Chen, J.H., Huang, Y., Brachi, B., et al., 2019. Genome-wide analysis of cushion willow provides insights into alpine plant divergence in a biodiversity hotspot. *Nat. Commun.* 10, 1–12.
- Darriba, D., Taboada, G.L., Doallo, R., et al., 2012. jModelTest 2: more models, new heuristics and high-performance computing Europe PMC Funders Group. *Nat. Methods* 9, 772.
- Dodd, A.N., Dalchau, N., Gardner, M.J., et al., 2014. The circadian clock has transient plasticity of period and is required for timing of nocturnal processes in *Arabidopsis*. *New Phytol.* 201, 168–179.
- Dodd, A.N., Salathia, N., Hall, A., et al., 2005. Cell biology: plant circadian clocks increase photosynthesis, growth, survival, and competitive advantage. *Science* 309, 630–633.
- Dogra, V., Li, Mingyue, Singh, S., Li, Mengping, Kim, C., 2019. Oxidative post-translational modification of EXECUTER1 is required for singlet oxygen sensing in plastids. *Nat. Commun.* 10, 1–12.
- Emms, D.M., Kelly, S., 2018. OrthoFinder2: fast and accurate phylogenomic orthology analysis from gene sequences. *BioRxiv* 466201.
- Emms, D.M., Kelly, S., 2015. OrthoFinder : solving fundamental biases in whole genome comparisons dramatically improves orthogroup inference accuracy. *Genome Biol.* 16, 157.
- Favre, A., Michalak, I., Chen, C.H., et al., 2016. Out-of-Tibet: the spatio-temporal evolution of *Gentiana* (Gentianaceae). *J. Biogeogr.* 43, 1967–1978.
- Frank, A., Mantioli, C.C., Viana, A.J.C., et al., 2018. Circadian entrainment in *Arabidopsis* by the sugar-responsive transcription factor bZIP63. *Curr. Biol.* 28, 2597–2606.
- Funk, W.C., Murphy, M.A., Hoke, K.L., et al., 2016. Elevational speciation in action? Restricted gene flow associated with adaptive divergence across an altitudinal gradient. *J. Evol. Biol.* 29, 241–252.
- Ge, X.J., Zhang, L.B., Yuan, Y.M., et al., 2005. Strong genetic differentiation of the east-himalayan *Megacodon stylophorus* (Gentianaceae) detected by inter-simple sequence repeats (ISSR). *Biodivers. Conserv.* 14, 849–861.
- Grudinski, M., Pannell, C.M., Chase, M.W., et al., 2014. An evaluation of taxonomic concepts of the widespread plant genus *Aglaia* and its allies across Wallace's Line (tribe Aglaieae, Meliaceae). *Mol. Phylogenet. Evol.* 73, 65–76.
- Guo, X., Hu, Q., Hao, G., et al., 2018. The genomes of two *Eutrema* species provide insight into plant adaptation to high altitudes. *DNA Res.* 25, 307–315.
- Hall, T.A., 1999. BioEdit: a user-friendly biological sequence alignment editor and analysis program for Windows 95/98/NT. In: *Nucleic Acids Symposium Series*, pp. 95–98.
- Hijmans, R.J., Cameron, S.E., Parra, J.L., Jones, P.G., Jarvis, A., 2005. Very high resolution interpolated climate surfaces for global land areas. *Int. J. Climatol.* 25, 1965–1978.
- Ho, T.N., Pringle, J.S., 1995. Gentianaceae. In: Wu, Z.-Y., Raven, P.H. (Eds.), *Flora of China*, vol. 16. Science Press and Missouri Botanical Garden, Beijing and St. Louis, pp. 1–139.
- Hoot, S.B., Culham, A., Crane, P.R., 1995. The utility of atpB gene sequences in resolving phylogenetic relationships: comparison with rbcL and 18S ribosomal DNA sequences in the Lardizabalaceae. *Ann. Mo. Bot. Gard.* 82, 194.
- Hudson, M.E., 2008. Sequencing breakthroughs for genomic ecology and evolutionary biology. *Mol. Ecol. Resour.* 8, 3–17.
- IUCN, 2012. In: IUCN Red List Categories and Criteria: Version 3.1, second ed. IUCN, Gland, Switzerland and Cambridge, UK. iv + 32pp.
- Jia, Y., Bai, J.Q., Liu, M.L., et al., 2019. Transcriptome analysis of the endangered *Notopterygium incisum*: cold-tolerance gene discovery and identification of EST-SSR and SNP markers. *Plant Divers* 41, 1–6.
- Johnson, C.D., Chary, S.N., Chernoff, E.A., et al., 2005. Protein geranylgeranyl-transferase I is involved in specific aspects of abscisic acid and auxin signaling in *Arabidopsis*. *Plant Physiol* 139, 722–733.
- Koops, P., Pelsler, S., Ignatz, M., et al., 2011. EDL3 is an F-box protein involved in the regulation of abscisic acid signalling in *Arabidopsis thaliana*. *J. Exp. Bot.* 62, 5547–5560.
- Lei, G.J., Zhu, X.F., Wang, Z.W., et al., 2014. Abscisic acid alleviates iron deficiency by promoting root iron reutilization and transport from root to shoot in *Arabidopsis*. *Plant Cell Environ.* 37, 852–863.
- Liu, C., Liao, Z.X., Liu, S.J., et al., 2014. Two new 2,3-seco-hopane triterpene derivatives from *Megacodon stylophorus* and their antiproliferative and antimicrobial activities. *Planta Med.* 80, 936–941.
- Löytynoja, A., Goldman, N., 2005. An algorithm for progressive multiple alignment of sequences with insertions. *Proc. Natl. Acad. Sci.* 102, 10557–10562.
- Luo, D., Xu, B., Li, Z.M., et al., 2017. The 'Ward Line–Mekong–Salween Divide' is an important floristic boundary between the eastern Himalaya and Hengduan mountains: evidence from the phylogeographical structure of subnival herbs *Marmoritis complanatum* (Lamiaceae). *Bot. J. Linn. Soc.* 185, 482–496.
- Ma, X.G., Sun, W.G., Zhu, W.D., et al., 2017. Resolving the phylogenetic relationships and evolutionary history of the East Asian endemic genus *Rodgersia* (Saxifragaceae) using multilocus data. *Perspect. Plant Ecol.* 25, 20–28.
- Ma, Y., Wang, J., Hu, Q., et al., 2019. Ancient introgression drives adaptation to cooler and drier mountain habitats in a cypress species complex. *Commun. Biol.* 2, 213.
- Marazzi, B., Bronstein, J.L., Koptur, S., 2013. The diversity, ecology and evolution of extrafloral nectaries: current perspectives and future challenges. *Ann. Bot.* 111, 1243–1250.
- Matuszak, S., Muellner-Riehl, A.N., Sun, H., et al., 2016. Dispersal routes between biodiversity hotspots in Asia: the case of the mountain genus *Tripterosperrum* (Gentianinae, Gentianaceae) and its close relatives. *J. Biogeogr.* 43, 580–590.
- Meng, L.H., Wang, Y., Luo, J., et al., 2012. Pollination ecology and its implication for conservation of an endangered perennial herb native to the East-Himalaya, *Megacodon stylophorus* (Gentianaceae). *Plant Ecol. Evol.* 145, 356–362.
- Miller, M.A., Pfeiffer, W., Schwartz, T., 2010. Creating the CIPRES Science Gateway for inference of large phylogenetic trees. In: 2010 Gateway Computing Environments Workshop (GCE), pp. 1–8.
- Missihoun, T.D., Willèe, E., Guegan, J.P., et al., 2014. Overexpression of *ALDH10A8* and *ALDH10A9* genes provides insight into their role in glycine betaine synthesis and affects primary metabolism in *Arabidopsis thaliana*. *Plant Cell Physiol.* 56, 1798–1807.
- Muellner-Riehl, A.N., Schnitzler, J., Kissling, W.D., et al., 2019. Origins of global mountain plant biodiversity: testing the 'mountain-geobiodiversity hypothesis'. *J. Biogeogr.* 46, 2826–2838.
- Myers, N., Mittermeier, R.A., Mittermeier, C.G., et al., 2000. Biodiversity hotspots for conservation priorities. *Nature* 403, 853–858.
- Qiao, Q., Wang, Q., Han, X., et al., 2016. Transcriptome sequencing of *Crucihimalaya himalaica* (Brassicaceae) reveals how *Arabidopsis* close relative adapt to the Qinghai-Tibet Plateau. *Sci. Rep.* 6, 1–8.

- Qin, F., Sakuma, Y., Tran, L.S.P., et al., 2008. *Arabidopsis* DREB2A-interacting proteins function as Ring E3 ligases and negatively regulate plant drought stress-responsive gene expression. *Plant Cell* 20, 1693–1707.
- R Core Team, 2018. R: A Language and Environment for Statistical Computing.
- Raychowdhury, R., Gnirke, A., Fan, L., et al., 2011. Full-length transcriptome assembly from RNA-Seq data without a reference genome. *Nat. Biotechnol.* 29, 644–652.
- Ronquist, F., Teslenko, M., Van Der Mark, P., et al., 2012. MrBayes 3.2: efficient Bayesian phylogenetic inference and model choice across a large model space. *Syst. Biol.* 61, 539–542.
- Sakata, T., Nakano, T., Yokoi, Y., 2006. Altitudinal changes in Rubisco and APX activities in *Aconogonum weyrichii* in the alpine region of Mt. Fuji. *Polar Biosci.* 115–122.
- Shrestha, N., Su, X., Xu, X., et al., 2018. The drivers of high *Rhododendron* diversity in south-west China: does seasonality matter? *J. Biogeogr.* 45, 438–447.
- Stamatakis, A., 2014. RAxML version 8: a tool for phylogenetic analysis and post-analysis of large phylogenies. *Bioinformatics* 30, 1312–1313.
- Strickler, S.R., Bombarely, A., Mueller, L.A., 2012. Designing a transcriptome next-generation sequencing project for a nonmodel plant species. *Am. J. Bot.* 99, 257–266.
- Sun, H., Zhang, J.W., Deng, T., et al., 2017. Origins and evolution of plant diversity in the Hengduan Mountains, China. *Plant Divers* 39, 161–166.
- Sun, Y.B., Fu, T.T., Jin, J.Q., et al., 2018. Species groups distributed across elevational gradients reveal convergent and continuous genetic adaptation to high elevations. *Proc. Natl. Acad. Sci.* 115, E10634–E10641.
- Supek, F., Bošnjak, M., Škunca, N., et al., 2011. Revigo summarizes and visualizes long lists of gene ontology terms. *PLoS One* 6.
- Suvorov, A., Jensen, N.O., Sharkey, C.R., et al., 2017. Opsins have evolved under the permanent heterozygote model: insights from phylotranscriptomics of *Odonata*. *Mol. Ecol.* 26, 1306–1322.
- Taberlet, P., Gielly, L., Pautou, G., et al., 1991. Universal primers for amplification of three non-coding regions of chloroplast DNA. *Plant Mol. Biol.* 17, 1105–1109.
- Thompson, J.D., Higgins, D.G., Gibson, T.J., 1994. Clustal W: improving the sensitivity of progressive multiple sequence alignment through sequence weighting, position-specific gap penalties and weight matrix choice. *Nucleic Acids Res.* 22, 4673–4680.
- Voelckel, C., Gruenheit, N., Lockhart, P., 2017. Evolutionary transcriptomics and proteomics: insight into plant adaptation. *Trends Plant Sci.* 22, 462–471.
- Wen, J., Zhang, J.Q., Nie, Z.L., et al., 2014. Evolutionary diversifications of plants on the Qinghai-Tibetan plateau. *Front. Genet.* 5, 1–16.
- Wu, Z.Y., 1988. Hengduan mountain flora and her significance. *J. Jpn. Bot.* 63, 297–311.
- Xie, C., Mao, X., Huang, J., et al., 2011. KOBAS 2.0: a web server for annotation and identification of enriched pathways and diseases. *Nucleic Acids Res.* 39, W316–W322.
- Xue, C.Y., Li, D.Z., 2005. Embryology of *Megacodon stylophorus* and *Veratrilla baillonii* (Gentianaceae): descriptions and systematic implications. *Bot. J. Linn. Soc.* 147, 317–331.
- Yang, Y., Karlson, D., 2013. AtCSP1 regulates germination timing promoted by low temperature. *FEBS Lett.* 587, 2186–2192.
- Yang, Z., 2007. PAML 4: phylogenetic analysis by maximum likelihood. *Mol. Biol. Evol.* 24, 1586–1591.
- Zhang, H., Ohyama, K., Boudet, J., et al., 2008. Dolichol biosynthesis and its effects on the unfolded protein response and abiotic stress resistance in *Arabidopsis*. *Plant Cell* 20, 1879–1898.
- Zhang, L., Yan, H.F., Wu, W., et al., 2013. Comparative transcriptome analysis and marker development of two closely related Primrose species (*Primula poissonii* and *Primula wilsonii*). *BMC Genom.* 14, 329.
- Zhang, T., Qiao, Q., Novikova, P.Y., et al., 2019. Genome of *Crucihimalaya himalaica*, a close relative of *Arabidopsis*, shows ecological adaptation to high altitude. *Proc. Natl. Acad. Sci.* 116, 7137–7146.
- Zhao, J.L., Gugger, P.F., Xia, Y.M., et al., 2016. Ecological divergence of two closely related *Roscoea* species associated with late Quaternary climate change. *J. Biogeogr.* 43, 1990–2001.